*Journal of University of Science and Technology Beijing*
*Vol.9(2002), No.1, p.48*

**Materials**

# A Novel Process for Synthesis of Ultrafine $BaTiO_3$ Powders

*Fangren Hu, Changchun Ge*

Laboratory of Special Ceramics and Powder Metallurgy,University of Science and Technology Beijing, Beijing 100083, China
(Received 2001-03-26)

**Abstract:** A novel process termed low-temperature combustion-synthesis (LCS) of $Ba(NO_3)_2$-$TiO_2$-$C_6H_8O_7 \cdot H_2O$ system was investigated at the initial temperature of 600 ℃ and ultrafine $BaTiO_3$ powders with a particle size of 200–350 nm were prepared. It was found that the molar ratio of $NO_3^-$/citric acid and the homogeneity of combustion have remarkable effect on the characteristics of the powder. The reaction mechanism of LCS $BaTiO_3$ powders was proposed on the basis of thermodynamic analysis.

**Key words:** low-temperature combustion-synthesis; barium titanate

## 1 Introduction

$BaTiO_3$ powder has a wide range of applications in the field of electric materials due to its excellent dielectric, piezoeletric, ferroeletric and electro-optic properties. The quality of the sintered $BaTiO_3$ specimens depends on the particle size, morphology, chemical purity and homogeneity, and stoichiometry of the starting powders. Hence processing routes for the synthesis of $BaTiO_3$ often have important effect on the properties of the sintered material.

In order to make high-quality powders, various synthesis processes such as solid-state mixed-oxide process, co-precipitation process, hydrothermal process, sol-gel process and other chemical processes have been used for preparing $BaTiO_3$ powders [1, 2]. However, these processes require multi-step routes with long-term reactions or expensive equipment and high energy consumption.

It is well known that high-temperature combustion-synthesis (CS) is an advanced powder preparation process. Earlier CS was mainly used for synthesizing non-oxide ceramics and intermetallics. In recent years, CS has been developed to synthesize oxide and complex oxide powders. A novel process termed low-temperature combustion-synthesis (LCS) derived from CS is developed to prepare ultrafine oxide powders [3].

LCS refers to a low-temperature self-sustaining combustion synthesis process in which oxidation-reduction reactions occur during heating the precursor derived from organic salt gel (or organic salt) and metal nitrate (or metal oxide). In contrast to other processes mentioned above, the following advantages of LCS are evident:

(1) Little energy is required to initiate a rapid reaction;

(2) Little or no further processing such as calcination and milling is required;

(3) Considerable savings in time, energy and equipment can be obtained;

(4) The process uses the heat generated by chemical reactions between fuel and precursors to convert metal ions into the target ceramic materials;

(5) Nano-oxides containing dopant elements, low temperature compounds and cermets, and complex-oxides with strict stoichiometry which are difficult to be synthesized by the conventional processes can be prepared;

(6) Ultrafine or nanopowders can be obtained in combination with wet chemical techniques, which allow the mixing degree of the reactants to be much better than by directly blending the solid reactants.

In this paper, ultrafine $BaTiO_3$ powders were synthesized by LCS. The combustion behavior of the Ba $(NO_3)_2$-$TiO_2$-$C_6H_8O_7 \cdot H_2O$ system and the effect of the molar ratio of $NO_3^-$/citric acid on the phase formation and powder characteristics were investigated.

## 2 Experimental Procedures

The raw materials $Ba(NO_3)_2$, $C_6H_8O_7 \cdot H_2O$ and $TiO_2$ used are reagent grade. The average particle size of $TiO_2$ is ~0.1 μm.

According to the propellant thermal-chemistry [3] and the following reaction:

Corresponding author: Fangren Hu
E-mail: Frhu@sina.com

$9Ba(NO_3)_2 + 9TiO_2 + 5C_6H_8O_7 \cdot H_2O \rightarrow 9BaTiO_3 + 30CO_2 + 9N_2 + 25H_2O$.

26.13 g $Ba(NO_3)_2$ was mixed stoichiometrically with $TiO_2$ and citric acid in an agate mortar. The mixture powders through −100 mesh were mixed homogeneously with 30 mL 65% $HNO_3$ (mass fraction) in a glass beaker, and heated in a furnace kept at 600 ℃, which smoked, bubbled and boiled after 2 min and lasted for 15 min followed with autoigniting yellow flame and large amount of gases. The combustion self-propagated from top to bottom of the glass beaker, lasted for 2 min and then extinguished. The combustion-synthesized powders (specimen A) are loose and porous, which are easy to be milled.

On the basis of the above-mentioned experiment, a series of specimens B1–B7 prepared from the mixtures of 26.13 g $Ba(NO_3)_2$ with different molar ratio of $NO_3^-$ / citric acid and 40 mL ethanol are shown in **table 1**.

**Table 1 Raw material compositions of the specimens**

| Specimen | Raw material compositions | | | | |
|---|---|---|---|---|---|
| | $m(Ba(NO_3)_2)$/g | $m(C_6H_8O_7 \cdot H_2O)$ / g | $m(TiO_2)$/g | $V_{Ethanol}$ / mL | Molar ratio of $NO_3^-$ / citric acid |
| B1 | 26.13 | 21.01 | 7.98 | 40 | 2.0:1 |
| B2 | 26.13 | 16.81 | 7.98 | 40 | 2.5:1 |
| B3 | 26.13 | 14.00 | 7.98 | 40 | 3.0:1 |
| B4 | 26.13 | 11.67 | 7.98 | 40 | 3.6:1 |
| B5 | 26.13 | 10.50 | 7.98 | 40 | 4.0:1 |
| B6 | 26.13 | 9.33 | 7.98 | 40 | 4.5:1 |
| B7 | 26.13 | 8.40 | 7.98 | 40 | 5.0:1 |

The mixtures were milled in a planetary mill for 6 h and then put into a furnace kept at 600 ℃ for LCS.

XRD was used for phase analysis, powder morphology was observed with SEM, agglomerated powder particle size was measured with SA-CP3 particle size analyzer, and specific surface of the as-prepared powders was measured with BET method.

## 3 Results and Discussions

SEM morphology of specimen A is shown in **figure 1**. Most of the powders with almost spherical morphology are agglomerated in different fashions throughout the sample. The agglomerates are basically clusters, each of which consists of some spherical powder particles. The characteristics of the powders in the clusters are uniform, weekly agglomerated with an average size of 1–2 μm and the clusters are easy to be deagglomerated by ultrasonic dispersion. The specific surfaces of the powders synthesized at the top, median and bottom zone of the glass beaker are 0.83 $m^2/g$, 0.76 $m^2/g$ and 0.70 $m^2/g$ respectively. The equivalent particle sizes calculated from specific surfaces are 1.21 μm, 1.32 μm and 1.43 μm respectively, consistent with the measured particle sizes from SEM morphology.

XRD analysis shows that the combustion synthesized powders at the top part of the glass beaker is Ba-

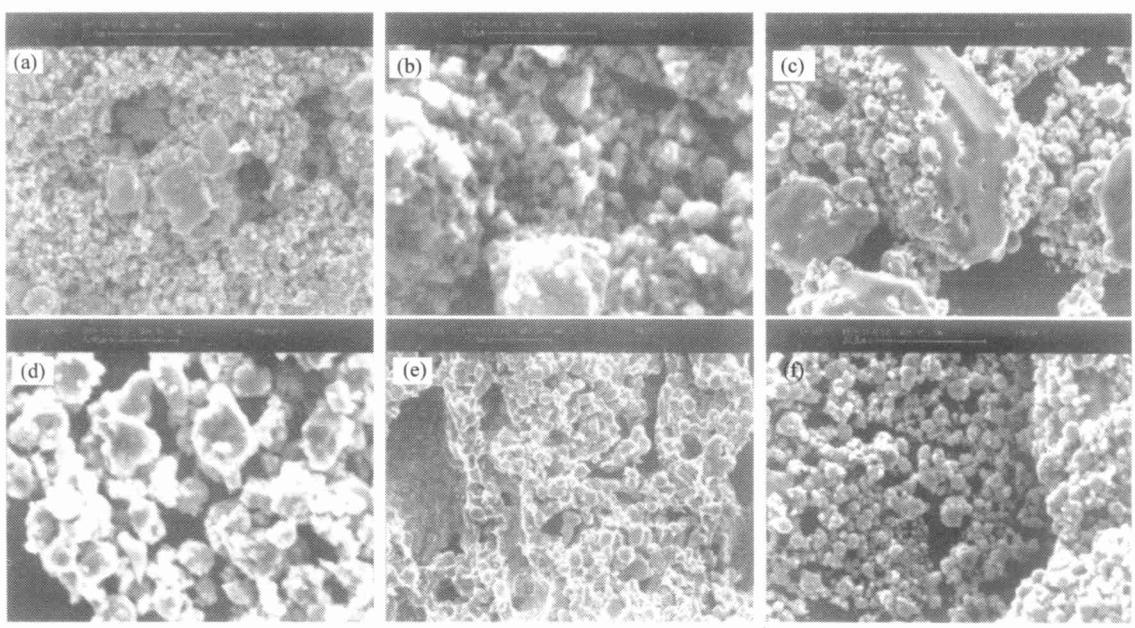


**Figure 1 SEM images of the as-synthesized $BaTiO_3$ powders of specimen A from different positions of the beaker after and before grinding respectively, (a) and (b) from the top zone; (c) and (d) from the median zone; (e) and (f) from the bottom zone.**

$TiO_3$ with a very small amount of $Ba_2Ti_9O_{20}$ and $BaCO_3$ as shown in **figure 2**. While more $Ba_2Ti_9O_{20}$ and $BaCO_3$ phases are formed at the median and bottom zones of the glass beaker. $Ba_2Ti_9O_{20}$ is beneficial for dielectric properties, while the small amount of $BaCO_3$ can be eliminated through a low temperature calcination.

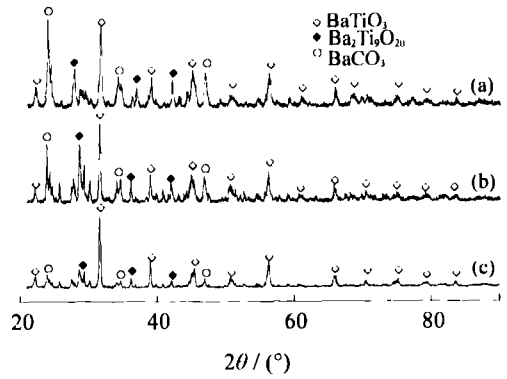


**Figure 2 XRD patterns of the combustion product from different zone of specimen A, (a) from the bottom zone; (b) from the median zone; (c) from the top zone.**

The molar ratio of $NO_3^-$/citric acid is an important factor of phase formation and morphology control of the as-synthesized powders. The mixture of specimens B1–B7 began to smoke, bubble and boil after being laid in the furnace for 30 s, continued for 2 min followed with autoigniting yellow flame and large amount of gases. The combustion flame lasted for 2–5 min and then extinguished.The XRD patterns (as shown in **figure 3**) of specimens B3, B4 and B5 show that the synthesized powder is $BaTiO_3$ with a very small amount of $Ba_2Ti_9O_{20}$ and $BaCO_3$, and the XRD patterns of B2 are of $BaTiO_3$ phase with only a very small amount of $Ba_2Ti_9O_{20}$ and no appearance of $BaCO_3$. While the XRD patterns of specimens B1, B6 and B7 show much more amount of $Ba_2Ti_9O_{20}$ and $BaCO_3$.

The specific surfaces of B2, B3 and B7 are 1.48, 2.48 and 0.98 $m^2/g$ respectively. The median agglomerated particle sizes of B2, B3 and B7 are 2.21, 0.65 and 2.95 μm respectively.The particle size distribution curves of specimens B2, B3 and B7 are shown in **figure 4**. SEM micrographs show spherical morphology with a particle size of 200–350 nm as shown in **figure 5**. Finer and more homogeneous powder with looser agglomeration is shown in the micrograph of B3 than that of B2 and B7, which is consistent with the results of agglomerated particle sizes and BET measurements.

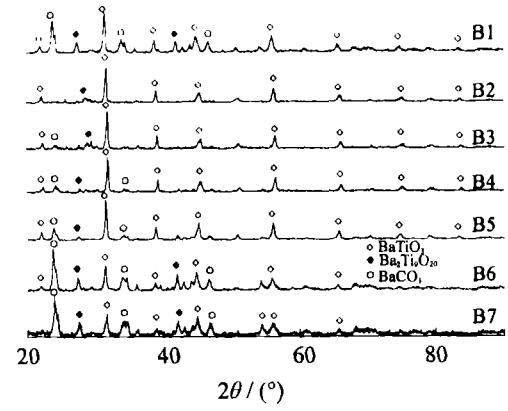


**Figure 3 XRD patterns of as-synthesized powders of specimens B1–B7.**

It is noticed that higher purity $BaTiO_3$ powders were obtained in stoichiometric (specimen B4), near stoichiometric (specimens B3, B5) composition or fuel-rich composition with the molar ratio of $NO_3^-$/citric acid of 2.5 (specimen B2) and the finest powder was obtained in specimen B3 with $d_{BET}=0.42$ μm ($d_{BET}$ is the equivalent particle size derived from the specific surface value). The lower $R_{d,B3}$ ratio of ~1.55 in specimen B3, in comparison with those of specimens B2 and B7 ($R_{d,B2}=3.25$, $R_{d,B7}=2.89$), indicates less and loose agglomerated powders in specimen B3, where $R_d$ is the ratio of median agglomerated particle size to BET equivalent particle size.

### 3.1 Mechanism of $BaTiO_3$ Formation

Two mechanisms have been proposed for $BaTiO_3$ formation from amorphous precursors [4]. One is that the precursors such as a citrate salt, $BaTi(C_6H_6O_7)_3 \cdot 6H_2O$ or an oxalate salt, $BaTiO(C_2O_4)_2 \cdot 4H_2O$, decompose to form a finely divided mixture of $BaCO_3$ and $TiO_2$, which subsequently reacts to form $BaTiO_3$ heated at 600–700 ℃. The other is that an intermediate basic carbonate forms during calcinations of citrate-based resins and oxalate salts with subsequent decomposition of the intermediate to $BaTiO_3$. On heating a mixed precursor for synthesis of $BaTiO_3$, if BaO crystallizes first, it can form any of the following phases: $BaTiO_3$, $BaCO_3$, and $Ba(OH)_2$ (**figure 6**). The formation of $Ba(OH)_2$ is least likely at all temperatures as shown in **figure 7**. At $1.01\times10^5$ Pa, $BaCO_3$ is the most stable phase until 172 ℃. If $BaCO_3$ crystallizes first, it will decompose into BaO and $CO_2$ when temperature > 893 ℃ in air. The formation of $BaTiO_3$ by a reaction between $BaCO_3$ and $TiO_2$ is thermodynamically possible when temperature >172 ℃ in a ir. However, $BaTiO_3$ is reported to form only when temperature >1 000 ℃ by the conventional solid-state mixed oxides process. Such a large difference may be due to the newly produced $BaCO_3$ or BaO and $TiO_2$ in the precursors are more active than those in the conventional solid-state mixed oxides process and the diffusion path between the newly produced $BaCO_3$ or BaO and $TiO_2$ in the precursors is shorter than that in the conventional solid-state mixed oxides process. Such a large difference in the thermodynamic feasibility and the actual formation tem-

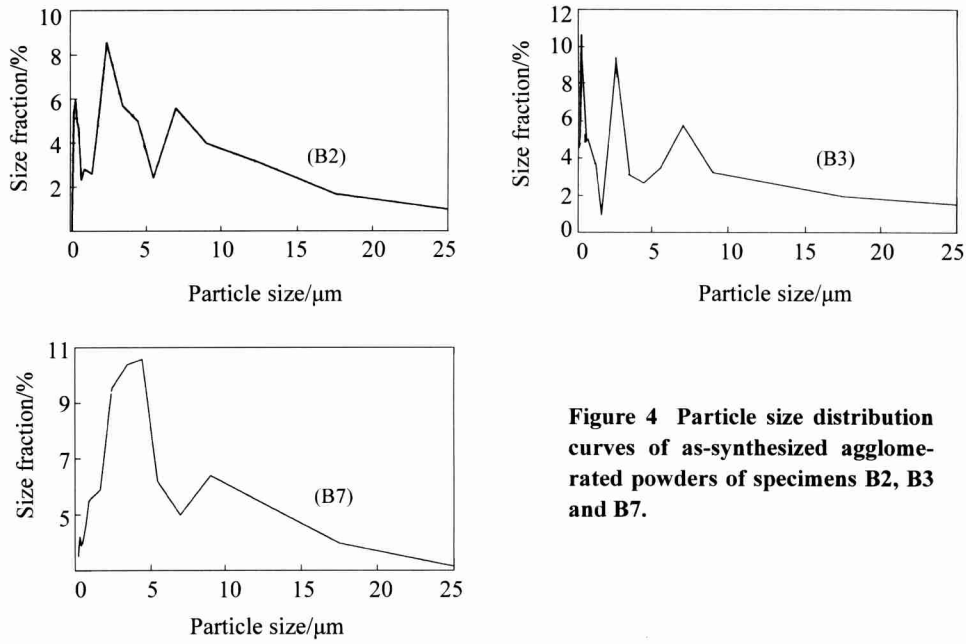


**Figure 4 Particle size distribution curves of as-synthesized agglomerated powders of specimens B2, B3 and B7.**

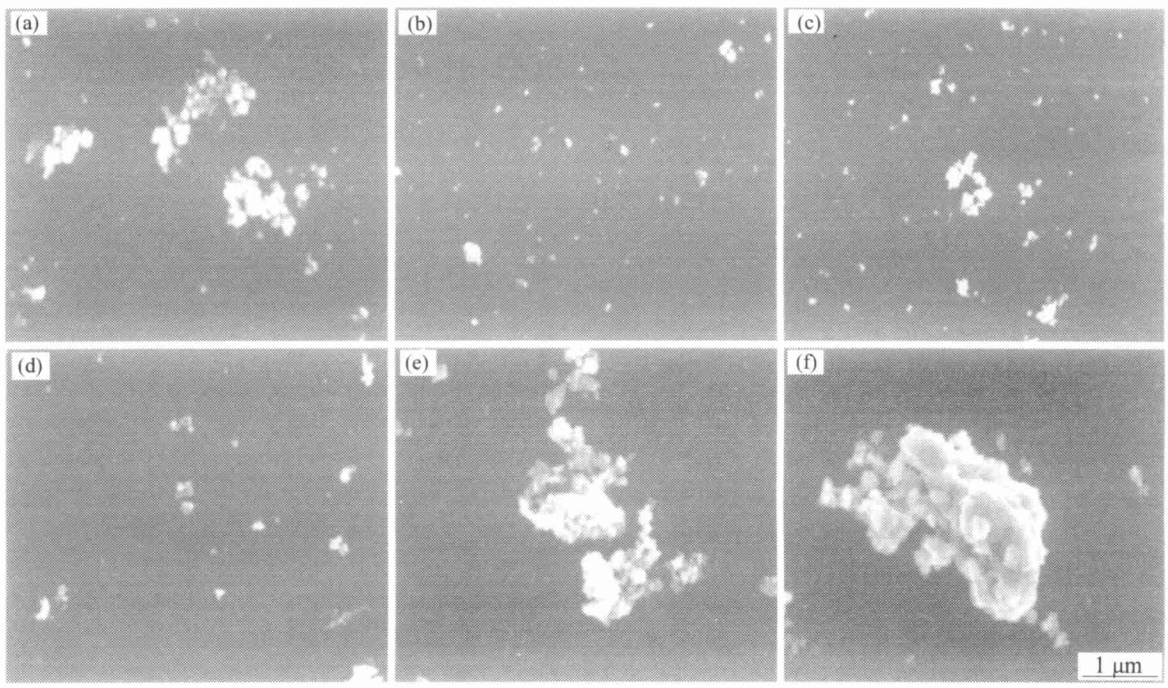


**Figure 5 SEM images of the as-synthesized powders of specimens (a) B1; (b) B2; (c) B3; (d) B4; (e) B5; (f) B7.**

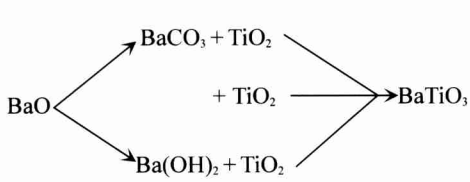


**Figure 6 Possible reactions starting with crystallization of BaO.**

peratures also indicates that this reaction in the conventional solid-state mixed oxides process is constrained by the kinetics and not thermodynamics.

According to F. R. Sale and F. Mahloojachi's work [4] on the barium nitrate-citric acid system, barium nitrate was detected, while no metastable citric salt was found. It is easy for nitrate to react with citric acid through the following exothermal reduction-oxidation

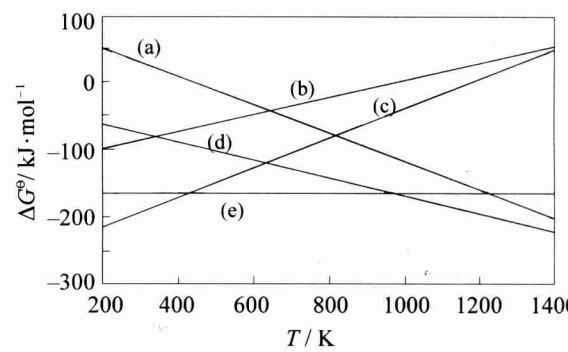


**Figure 7 $\Delta G^{\ominus}$ vs $T$ at $1.01\times10^5$ Pa, (a) $BaCO_3+TiO_2\rightarrow BaTiO_3+CO_2\uparrow$; (b) $BaO+H_2O\rightarrow Ba(OH)_2$; (c) $BaO+CO_2\rightarrow BaCO_3$; (d) $Ba(OH)_2+TiO_2\rightarrow BaTiO_3+CO_2\uparrow$; (e) $BaO+TiO_2\rightarrow BaTiO_3$.**

reaction during heating:

$$9Ba(NO_3)_2 + 5C_6H_8O_7 \cdot H_2O \rightarrow 30CO_2 + 9N_2 + 25H_2O + 9BaO \quad (1)$$

Tsang-Tse Fang [5] reported that $Ba(NO_3)_2$ would decompose at 400-600℃:

$$Ba(NO_3)_2 \rightarrow BaO + 2NO_2 + \frac{1}{2}O_2 \quad (2)$$

As seen in figure 7, $BaCO_3$ is the most stable compound at $1.01\times10^5$ Pa until 172℃ in the Ba-Ti-C-O-H system [6]:

$$BaO + CO_2 \rightarrow BaCO_3 \quad (3)$$

With increasing temperature, the stability of $BaCO_3$ decreased and $BaTiO_3$ would form from the unreacted BaO through the following reaction:

$$BaO + TiO_2 \rightarrow BaTiO_3 \quad (4)$$

This reaction is insensitive to temperature change.

In presence of $TiO_2$, $BaCO_3$ will react with $TiO_2$ to form $BaTiO_3$ through the following reaction above 172℃:

$$BaCO_3 + TiO_2 \rightarrow BaTiO_3 + CO_2 \quad (5)$$

In the $Ba(NO_3)_2$-$TiO_2$-$C_6H_8O_7 \cdot H_2O$ system, the main reactions occurring in the higher temperature flame zone might be reactions (1), (4) and (5), while those occurring in medium and low temperature zone might be (1), (2), (3) and (5), and $Ba_2Ti_9O_{20}$ formed through:

$$2BaCO_3 + 9TiO_2 \rightarrow Ba_2Ti_9O_{20} + 2CO_2 \quad (6)$$

According to the above-mentioned analysis, it can be understood that $BaTiO_3$ decreased while $BaCO_3$ and $Ba_2Ti_9O_{20}$ increased in the combustion product from top to bottom of the glass beaker, as shown in the XRD patterns in figure 2. It would be beneficial for eliminating $BaCO_3$ through increasing the combustion temperature and creating a homogeneous combustion zone. It is obvious that inhomogeneous combustion causes inhomogeneity of particle sizes, specific surfaces, porosity and agglomeration states of powders in different zones. Due to higher combustion temperature of the precursor at the top of the glass beaker, more complete combustion and more gases evolved lead to the higher content of $BaTiO_3$, finer particle size, higher specific surface and higher porosity of powder agglomerates, in comparison with those at the medium and bottom parts of the glass beaker, which is consistent with the SEM images in figure 1.

The effect of the molar ratio of $NO_3^-$/citric acid on the powder characteristics can also be explained from the above-mentioned analysis. When the molar ratio of $NO_3^-$/citric acid = 2.5–3.0, there occurred sufficient oxidation-reduction reaction in the system, in which $Ba(NO_3)_2$ decomposed and evolved $NO_2$. $NO_2$ reacted with citric acid to produce large quantity of heat and gases, and resulted in higher content of $BaTiO_3$ and specific surfaces of powders.As the molar ratio of $NO_3^-$ /citric acid increased from 2.5 to 5.0, or decreased from 2.5 to 2.0, insufficient oxidation or reduction causes incomplete combustion, lower combustion temperatures, lower content of $BaTiO_3$ and specific surfaces of powders.

In order to synthesize high purity, mono-phase $BaTiO_3$ powder, a precursor with the compositions mixed in the level of atom or molecule is needed. The LCS of $Ba(NO_3)_2$-$TiO_2$-$C_6H_8O_7 \cdot H_2O$ system is to be investigated and the control of homogeneous and complete combustion is to be proceeded.

## 4 Conclusions

LCS of $Ba(NO_3)_2$-$TiO_2$-$C_6H_8O_7 \cdot H_2O$ system was investigated and ultrafine $BaTiO_3$ powders with particle size of 200–350 nm were synthesized. It is found that the molar ratio of $NO_3^-$/citric acid and the homogeneity of combustion have important effect on the phase formation and powder characteristics. The reaction mechanism of LCS $BaTiO_3$ powders was proposed based on thermodynamic analysis and experimental results. Further work is to be proceeded to obtain a homogeneous precursor with the compositions mixed in a level of atom or molecule and homogeneous and complete combustion for synthesizing high purity and mono-dispersed $BaTiO_3$ nanopowder.

## References

[1] Pradeep P. Phule, Subhash H. Risbud. *J. Mater. Sci.* [J]. 25 (1990), p. 1169.

[2] A. D. Hilton, R. Frost. *Key Engin Mater* [J]. 66-67 (1992), p. 145.

[3] W. X. Li, S. Yin. *Journal of Silicate* [J]. 27 (1999), No.1, p. 1.

[4] F. R. Sale, F. Mahloojachi: *Ceram Inter* [J]. 14 (1988), p. 229.

[5] Tsang-Tse Fang, Horng-Bin Lin, Jim-Bin Hwang. *J. Am. Ceram. Soc.* [J]. 73 (1990), No. 11, p. 3363.

[6] Suresh Kumar, Gary L. Messing, William B. White. *J. Am. Ceram. Soc.* [J]. 76 (1993), No.3, p. 617.